

Josephson-current induced conformational switching of a molecular quantum dot

A. Zazunov, A. Schulz, and R. Egger

Institut für Theoretische Physik, Heinrich-Heine-Universität, D-40225 Düsseldorf, Germany

(Dated: November 17, 2018)

We discuss the behavior of a two-level system coupled to a quantum dot contacted by superconducting source/drain electrodes, representing a simple model for the conformational degree of freedom of a molecular dot or a break junction. The Josephson current is shown to induce conformational changes, including a complete reversal. For small bias voltage, periodic conformational motions induced by Landau-Zener transitions between Andreev states are predicted.

PACS numbers: 74.50.+r, 74.78.Na, 73.63.-b

The remarkable recent progress in the fabrication and experimental study of transport through ultrasmall nanoscopic devices, break junctions, or molecules (in the following termed “quantum dot” or simply “dot”) [1] has stimulated renewed interest in the Josephson effect [2], where the Josephson current through a dot contacted by superconducting electrodes with phase difference φ is the relevant observable. The full current-phase relation has been measured in various systems, and electron-electron interactions on the dot were shown to be important [3], as expected from theory [4]. The already achieved wide tunability (via gate electrodes) and impressive control over Josephson currents through nanoscale dots indicate that experiments should be able to also probe modifications of the super-current due to the coupling of the dot to another quantum system (e.g., a spin or a side-coupled dot). Many previous efforts have focussed on studying the coupling to the spin degree of freedom in molecular magnets [5], which is also related to issues appearing for superconductor-ferromagnet-superconductor structures [6]. Theoretical work has also discussed the effects of local vibration modes on the super-current, where the dot is coupled to a boson mode (phonon) [7, 8].

Surprisingly, so far the effects of a *two-level system* (TLS) coupled to the dot have not been addressed, except for normal-conducting leads. This is an important question, since for instance two *conformational configurations* of a molecule may represent the TLS degree of freedom. Experimental results for molecular dots or break junctions (with normal leads) were interpreted along this line [9, 10, 11, 12], but a TLS can also be realized for a side-coupled double-dot system in the Coulomb blockade regime [13]. For concreteness, we here refer to the TLS states $\sigma_z = \pm 1$ as the two distinct conformational states of a molecular dot, where σ_z couples to the dot’s charge. A coupling of the TLS to the dot’s spin does not have a significant effect on the phenomena of interest here, see below. (In any case, spin effects have been addressed in different contexts previously [5].) Our theory indicates that by variation of the phase φ , the TLS state can be significantly affected over a wide parameter regime, including a complete reversal of the conformational configuration. This remarkable effect allows for the dissipationless control (including switching) of the conformational degree of freedom (σ_z) in terms of the

phase difference φ , which can be tuned experimentally by embedding the device in a SQUID geometry [3]. Conversely, changing the conformational state will affect the Josephson current in a distinct manner. Moreover, when applying a bias voltage, a periodic conformational motion is triggered via the ac Josephson effect involving Landau-Zener (LZ) transitions between Andreev states. Our predictions (both for zero and finite bias) can be tested experimentally for a wide class of molecules electrically contacted in a break junction setup. Related experiments, reporting TLS behavior due to a conformational variable, have been published for normal leads [9]. For normal leads, the model employed below has also been motivated in a recent theoretical work [12]. Available parameter estimates for dot and TLS energy scales [9, 12] suggest that the predicted phenomena can be observed using existing state-of-the-art experiments. Detection schemes to read out the conformational state are also available, e.g. by single-molecule force microscopy [14].

We study a spin-degenerate molecular dot level with single-particle energy ϵ_d and on-site Coulomb repulsion $U > 0$, coupled to the TLS and to two superconducting banks (leads). Employing the standard wide-band approximation for the leads, we assume a symmetric situation [15], where the banks are modelled as identical *s*-wave BCS superconductors with gap Δ and the dot-lead hybridizations are equal, $\Gamma_L = \Gamma_R = \Gamma/2$. The TLS describing the conformational state corresponds to Pauli matrices $\sigma_{x,z}$, with bare energy difference E_0 and tunnel matrix element W_0 between the two states. The Hamiltonian is $H = H_0 + H_{\text{tun}} + H_{\text{leads}}$, where the coupled dot-plus-TLS part is (we set $e = \hbar = k_B = 1$)

$$H_0 = -\frac{E_0}{2}\sigma_z - \frac{W_0}{2}\sigma_x + \left(\epsilon_d + \frac{\lambda}{2}\sigma_z\right)(n_\uparrow + n_\downarrow) + Un_\uparrow n_\downarrow, \quad (1)$$

with the occupation number $n_s = d_s^\dagger d_s$ for the dot fermion d_s with spin $s = \uparrow, \downarrow$, H_{leads} describes standard BCS Hamiltonians, φ can be included by phase factors in the tunnel Hamiltonian H_{tun} [8], and we define the renormalized dot level $\epsilon = \epsilon_d + U/2$. In Eq. (1), the TLS couples with strength λ to the charge on the dot, which can be rationalized in simple terms by assuming a one-dimensional effective reaction coordinate X describing conformations

of the molecule. The dominant coupling to the electronic degrees of freedom is then (as for phonons) of the form $\propto X(n_\uparrow + n_\downarrow)$ [7, 8, 9, 10]. In the limit of interest, the potential energy $V(X)$ is bistable with two local minima, and a truncation of the low-energy dynamics of X to the lowest quantum state in each well leads to Eq. (1). For a detailed derivation, see also Ref. [12].

When dealing with the equilibrium problem, it is convenient to work with Nambu spinors $d(\tau) = (d_\uparrow, d_\downarrow^\dagger)$ in imaginary time τ . The lead fermions can then be integrated out exactly, and the partition function is $Z = \text{Tr} \left(e^{-H_0/T} \mathcal{T} e^{-\int d\tau d\tau' d^\dagger(\tau) \Sigma(\tau-\tau') d(\tau')} \right)$, where the trace extends over the dot-plus-TLS degrees of freedom only, \mathcal{T} denotes time-ordering, and the effect of the BCS leads is contained in the 2×2 Nambu self-energy matrix $\Sigma(\tau)$, whose Fourier transform is [4]

$$\Sigma(\omega; \varphi) = \frac{\Gamma}{\sqrt{\omega^2 + \Delta^2}} \begin{pmatrix} -i\omega & \Delta \cos(\varphi/2) \\ \Delta \cos(\varphi/2) & -i\omega \end{pmatrix}. \quad (2)$$

We mostly consider zero temperature, $T = 0$, where both the Josephson current $I(\varphi)$ through the dot and the expectation value $S = \langle \sigma_z \rangle$ of the conformational state follow from the ground-state energy $E_g(\varphi, E_0)$ according to

$$I(\varphi) = 2 \frac{\partial E_g}{\partial \varphi}, \quad S(\varphi) = -2 \frac{\partial E_g}{\partial E_0}. \quad (3)$$

Later on the formalism will be extended along the lines of Refs. [16, 17] to allow for the description of a small bias voltage V as well.

Let us first illustrate our central findings when both the charging energy U and the tunnel splitting W_0 are very small. Later on we show that for sufficiently small $U < U_c$, finite U has no effect. The ground-state energy $E_g = \min(E_+, E_-)$ then follows from the energies $E_\sigma = \sigma(\lambda - E_0)/2 - \epsilon_\sigma^A(\varphi)$ for fixed conformational state $\sigma = \pm$ with dot level $\epsilon_\sigma = \epsilon + \sigma\lambda/2$. With Eq. (2) and $\tau_z = \text{diag}(1, -1)$, the *Andreev state* energy for arbitrary Δ/Γ follows from

$$\epsilon_\sigma^A(\varphi) = \epsilon_\sigma^A(0) + \int \frac{d\omega}{2\pi} \ln \frac{\det [i\omega - \tau_z \epsilon_\sigma - \Sigma(\omega; \varphi)]}{\det [i\omega - \tau_z \epsilon_\sigma - \Sigma(\omega; 0)]}. \quad (4)$$

In the limits $\Gamma \gg \Delta$ and $\Delta \gg \Gamma$, this yields [2]

$$\begin{aligned} \epsilon_\sigma^A(\varphi) &= \Delta_\sigma \sqrt{1 - \mathcal{T}_\sigma \sin^2(\varphi/2)}, \\ \Delta_\sigma &= \begin{cases} \frac{\Delta}{1 + \Delta/\Gamma}, & \Gamma \gg \Delta, \\ \frac{\Gamma}{\sqrt{\mathcal{T}_\sigma}}, & \Delta \gg \Gamma, \end{cases} \end{aligned} \quad (5)$$

with the normal transmission probability $\mathcal{T}_\sigma = [1 + \epsilon_\sigma^2/\Gamma^2]^{-1}$. As long as $E_+ < E_-$ ($E_- < E_+$), we have $S(\varphi) = +1(-1)$, i.e. the conformational state $\sigma = +(-)$ is realized, with ideal (perfect) switching when the bands $E_+(\varphi)$ and $E_-(\varphi)$ cross at some phase $0 < \varphi^* < \pi$. Hence a necessary condition for switching follows: one of the two inequality chains (with $\mathcal{R}_\sigma = 1 - \mathcal{T}_\sigma$)

$$\Delta_+ \sqrt{\mathcal{R}_+} - \Delta_- \sqrt{\mathcal{R}_-} \lesssim \lambda - E_0 \lesssim \Delta_+ - \Delta_- \quad (6)$$

must be obeyed. If the dot level is close to a resonance, $\epsilon_+ \approx 0$ or $\epsilon_- \approx 0$, the reflection probabilities \mathcal{R}_+ and \mathcal{R}_- are significantly different, and Eq. (6) holds over a wide parameter range. Then Eq. (3) yields

$$I(\varphi) = \frac{e\Delta_{S(\varphi)}}{2\hbar} \frac{\mathcal{T}_{S(\varphi)} \sin(\varphi)}{\sqrt{1 - \mathcal{T}_{S(\varphi)} \sin^2(\varphi/2)}}. \quad (7)$$

In the regime (6), the transmission amplitude switches between \mathcal{T}_+ and \mathcal{T}_- when $\varphi = \varphi^*$. This implies non-standard current-phase relations, as shown in the upper inset of Fig. 1.

Having established the basic phenomenon, we now address the effects of finite U and/or tunneling W_0 . Progress can be made in the limits $\Gamma \gg \Delta$ and $\Delta \gg \Gamma$. Let us start with the case when Δ is the largest energy scale of relevance. Then the dynamics is always confined to the subgap regime (Andreev states), and quasi-particle tunneling processes from the leads (continuum states) are negligible. Technically, Eq. (2) can then be replaced by $\Sigma(\tau) = \Gamma \cos(\varphi/2) \delta(\tau) \begin{pmatrix} 0 & 1 \\ 1 & 0 \end{pmatrix}$, and the problem is equivalently described by the effective Hamiltonian $H_{\text{eff}} = H_0 + \Gamma \cos(\varphi/2) (d_\downarrow d_\uparrow + d_\uparrow^\dagger d_\downarrow^\dagger)$. The resulting Hilbert space can be decomposed into orthogonal subspaces, $\mathcal{H} = \mathcal{H}_A \otimes \mathcal{H}_S$, where the Andreev sector \mathcal{H}_A is spanned by the zero- and two-electron dot states $|0\rangle$ and $|2\rangle = d_\uparrow^\dagger d_\downarrow^\dagger |0\rangle$ (and, of course, by the conformational TLS states), while \mathcal{H}_S is spanned by the one-electron states $|s\rangle \equiv d_s^\dagger |0\rangle$. For convenience shifting $H_{\text{eff}} \rightarrow H_{\text{eff}} - \epsilon$, the single-particle sector has a pair of doubly-degenerate eigenenergies $-\frac{U}{2} \pm \epsilon_S$ with $\epsilon_S = \frac{1}{2} \sqrt{(E_0 - \lambda)^2 + W_0^2}$, whereas the Andreev sector is described by

$$H_{\text{eff}}^A = \frac{\lambda - E_0}{2} \sigma_z - \frac{W_0}{2} \sigma_x + \frac{\lambda}{2} \tau_z \sigma_z + \epsilon \tau_z + \Gamma \cos(\varphi/2) \tau_x \quad (8)$$

with Pauli matrices $\tau_{x,z}$ acting in $\{|2\rangle, |0\rangle\}$ subspace. If the ground state of H_{eff} lies in the Andreev sector, the Josephson current can be non-zero, while otherwise $I = 0$ due to the φ -independence of the single-particle sector. For sufficiently strong interactions, $U > U_c(\varphi)$, the ground state of H_{eff} is in the single-particle sector \mathcal{H}_S . This is indicative of a quantum phase transition to the magnetic π -junction regime [4]. While this regime is outside the scope of Eq. (8) (since continuum states are not included), we have confirmed this scenario by a perturbative calculation expanding in Γ for the full model. For $\lambda \rightarrow 0$, we find $U_c = 2\sqrt{\epsilon^2 + \Gamma^2 \cos^2(\varphi/2)}$, see Eq. (5) for $\Delta \gg \Gamma$. Note that ϵ and hence U_c can in principle be tuned by a gate voltage. For $\lambda \gg \max(|E_0|, |\epsilon|, \Gamma)$, we instead find $U_c = \lambda$. Because H_{eff}^A is independent of U (up to the shift $\epsilon = \epsilon_d + U/2$), a weak interaction $U < U_c$ has no effect, and in what follows we set $U = 0$. Since a coupling of the TLS to the dot's *spin* involves only the φ -independent subspace \mathcal{H}_S , such couplings are also of little relevance for switching, in accordance with

the small polar displacements predicted for spins in a Josephson junction [5].

Physical observables can then be computed from H_{eff}^A in Eq. (8). The eigenenergies are roots to the exactly solvable quartic equation

$$E^4 - 2\Lambda_2 E^2 + \Lambda_1 E + \Lambda_0 = 0, \quad (9)$$

with coefficients $\Lambda_2 = \epsilon_A^2 + \epsilon_S^2 + \lambda^2/4$, $\Lambda_1 = 2\lambda\epsilon(E_0 - \lambda)$ and $\Lambda_0 = (\epsilon_A^2 - \epsilon_S^2 + \lambda^2/4)^2 - \lambda^2(\epsilon^2 - W_0^2/4)$. The lowest-lying of the four roots yields the exact but lengthy result for the ground-state energy E_g . Convenient expressions for $S(\varphi)$ and $I(\varphi)$ in Eq. (3) follow by taking the respective derivatives directly in Eq. (9). For instance, with $\Lambda'_i = \partial\Lambda_i/\partial E_0$, the conformational variable reads

$$S(\varphi) = -\frac{2\Lambda'_2 E_g^2 - \Lambda'_1 E_g - \Lambda'_0}{2E_g(E_g^2 - \Lambda_2) + \Lambda_1/2}. \quad (10)$$

Typical results for $S(\varphi)$ and $I(\varphi)$ are shown in Fig. 1. The most efficient way to induce conformational changes, including a complete (symmetric) reversal $S \rightarrow -S$, is achieved in the weak-coupling regime $\lambda \ll \epsilon_A$, where the four roots to Eq. (9) can be simplified to

$$E_{\pm, \pm} = \pm\epsilon_A(\varphi) \pm \frac{1}{2}\sqrt{W_0^2 + [\lambda(1 - \epsilon/\epsilon_A(\varphi)) - E_0]^2}, \quad (11)$$

with ground-state energy $E_g = E_{--}$. Remarkably, Eq. (11) remains accurate even for $\lambda \approx \epsilon_A$. A complete reversal is achieved when tuning E_0 or ϵ such that $E_0 = \lambda[1 - \text{sgn}(\epsilon)] - \mathcal{F}$ with $\mathcal{F} = -\frac{\lambda}{2}\text{sgn}(\epsilon)[1 - |\epsilon|/\epsilon_A(0)]$. In that case, $S(0) = -S(\pi) = \mathcal{F}/\sqrt{W_0^2 + \mathcal{F}^2}$. When comparing to the $W_0 = 0$ result, we observe that a finite tunnel amplitude W_0 only leads to a rounding of the transition and a decrease in the switching amplitude, but it does not destroy the effect. Finally, with Eq. (11), the Josephson current in the weak-coupling limit is

$$I(\varphi) = \frac{\Gamma^2 \sin \varphi}{2\epsilon_A(\varphi)} \left(1 + \frac{\lambda\epsilon}{2\epsilon_A^2(\varphi)} S(\varphi) \right). \quad (12)$$

Next we briefly discuss the opposite limit within a similar truncation scheme, setting $U = 0$. For $\Gamma \gg \Delta$ and $\varphi \neq 2\pi n$ (integer n), the relevant subgap dynamics is again captured by an effective two-level Hamiltonian describing the Andreev states [18], coupled to the conformational TLS. With Pauli matrices $\tau_{x,y,z}$ in Andreev level subspace and the notation [see Eq. (5)]

$$H_\sigma = \Delta_\sigma e^{-i\tau_y \sqrt{R_\sigma} \varphi/2} \left(\sqrt{R_\sigma} \sin(\varphi/2) \tau_z + \cos(\varphi/2) \tau_x \right),$$

the effective Hamiltonian follows in TLS space as

$$H_{\text{eff}} = \begin{pmatrix} \frac{\lambda - E_0}{2} + H_+ & -\frac{W_0}{2} \\ -\frac{W_0}{2} & -\frac{\lambda - E_0}{2} + H_- \end{pmatrix}. \quad (13)$$

Physical observables are then easily obtained, see the lower inset of Fig. 1. Again the qualitative features of the $W_0 = 0$ solution persist.

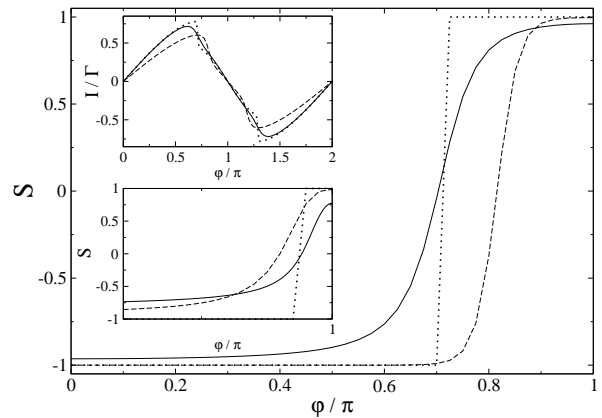


FIG. 1: Conformational state $S(\varphi) = S(-\varphi)$ vs superconductor's phase difference φ . Results from Eq. (10) for $\Delta \gg \Gamma$ are shown for tunnel amplitudes $W_0 = 0$ (dotted) and $W_0 = 0.04\Gamma$ (solid), with $\lambda = \epsilon = \Gamma/2$ and $E_0 = 0.14\Gamma$. The dashed curve gives the exact result for $W_0 = 0$ and $\Delta = 5\Gamma$, see Eq. (4), extended to finite temperature $T = 0.01\Gamma$. The upper inset shows the corresponding Josephson current-phase relations. Lower inset: Same as main figure but for $\Gamma = 4\Delta$ with $\lambda = 2\epsilon = \Delta/2$ and $E_0 = 0.45\Delta$. The dotted (solid) curve is obtained from the $\Gamma \gg \Delta$ effective Hamiltonian (13) with $W_0 = 0$ ($W_0 = 0.04\Delta$). The exact result for $W_0 = 0$ is shown as dashed curve for $T = 0.01\Delta$.

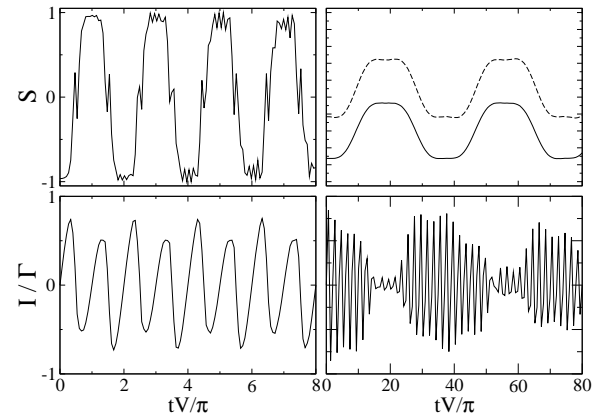


FIG. 2: Time dependence of S (upper row) and ac Josephson current I (lower row). The left panel shows the adiabatic evolution for low voltage, $V = 0.01\Gamma$. Parameters are the same as for the solid curve in the main panel of Fig. 1. The right panel is for $V = 5\Gamma$ with $\epsilon/\Gamma = 0.2$ (solid) and 0.6 (dashed, current not shown). Other parameters are $\lambda = \Gamma/2$ and $E_0 = W_0 = 0.2\Gamma$.

The effective Hamiltonian (8) for $\Delta \gg \Gamma$ also allows to study the voltage-biased junction with $V \ll \Delta$, where the superconducting phase difference is time-dependent, $\varphi(t) = 2Vt$. During the time evolution induced by $\varphi(t)$, the Andreev and single-particle Hilbert subspaces \mathcal{H}_A and \mathcal{H}_S remain decoupled and mutually orthogonal. The task is therefore reduced to solving the time-dependent Schrödinger equation $i\partial_t \Psi(t) = H_{\text{eff}}^A(t) \Psi(t)$, where $\Psi(t)$ is a 4-component wave function representing the two An-

dreev states and the TLS, and $H_{\text{eff}}^A(t)$ is given by Eq. (8) with $\varphi \rightarrow 2Vt$. For this description to hold at finite Δ , the escape rate γ of Andreev state quasiparticles into the continuum states of the leads should be negligibly small. The rate γ follows from the tunneling self-energy, see Ref. [17] for the opposite limit $\Gamma \gg \Delta$. For $\epsilon = 0$, we find

$$\gamma \simeq \Gamma \exp\left(-\frac{2\Delta}{V} [\ln(2\Delta/\Gamma) - 1]\right), \quad (14)$$

leading to exponentially small rates for realistic system parameters throughout the regime $\Delta \gg \Gamma$. Numerical solution of the time-dependent Schrödinger equation leads to the results in Fig. 2. They can be understood in terms of the four eigenenergies (11). For small V , the time evolution is basically adiabatic, and the LZ probability is very small. The left panel in Fig. 2 shows such an adiabatic evolution involving time-periodic level crossings of the bands E_{--} and E_{-+} in Eq. (11), thereby explaining the existence of two different supercurrent oscillation amplitudes. The “noisy” features in $S(t)$ are fully reproducible and reflect a superposition of almost filled and almost empty levels. There are no LZ transitions in that limit, but only a continuous change of energy bands at

the branching times where $E_{--} = E_{-+}$. However, for larger V/Γ , the LZ probability becomes sizeable and the dynamics is more complex, generally involving a dynamical population of all four subgap states. The right panel in Fig. 2 displays the case of relatively large V , where the system oscillates due to LZ transitions between the levels E_{--} and E_{-+} . The frequency ω_S of the $S(t)$ oscillations is much slower than the Josephson frequency $\omega_J = 2eV/\hbar$ and determined by the lowest interlevel transition energy, $\omega_S = \min(E_{-+} - E_{--})$. Note that ω_S reappears in the ac Josephson current.

To conclude, we predict that the conformational degree of freedom (represented by a TLS) in a superconducting molecular dot or break junction responds in a dissipationless manner to variations of the phase difference φ across the dot/junction, including a complete reversal. This effect should be observable using existing experimental methods over a wide parameter range. Under an applied voltage, this effect leads to quasi-periodic TLS dynamics due to the time-dependent occupation probabilities of Andreev states.— We thank T. Martin for discussions. This work was supported by the SFB TR 12 of the DFG and by the EU networks INSTANS and HYSWITCH.

-
- [1] N.J. Tao, *Nature Nanotechnology* **1**, 173 (2006).
 [2] A.A. Golubov, M.Yu. Kupriyanov, and E. Il'ichev, *Rev. Mod. Phys.* **76**, 411 (2004).
 [3] See, for instance, J.A. van Dam *et al.*, *Nature (London)* **442**, 667 (2006); M.L. Della Rocca *et al.*, *Phys. Rev. Lett.* **99**, 127005 (2007).
 [4] L.I. Glazman and K.A. Matveev, *JETP Lett.* **49**, 659 (1989); A.V. Rozhkov and D.P. Arovav, *Phys. Rev. Lett.* **82**, 2788 (1999); E. Vecino, A. Martín-Rodero, and A.L. Yeyati, *Phys. Rev. B* **68**, 035105 (2003); F. Siano and R. Egger, *Phys. Rev. Lett.* **93**, 047002 (2004); M.S. Choi, M. Lee, K. Kang, and W. Belzig, *Phys. Rev. B* **70**, 020502(R) (2004).
 [5] J.X. Zhu, Z. Nussinov, A. Shnirman, and A.V. Balatsky, *Phys. Rev. Lett.* **92**, 107001 (2004); Z. Nussinov *et al.*, *Phys. Rev. B* **71**, 214520 (2005); M. Lee, T. Jonckheere, and T. Martin, *Phys. Rev. Lett.* **101**, 146804 (2008).
 [6] A.I. Buzdin, *Rev. Mod. Phys.* **77**, 935 (2005); F.S. Bergeret, A.F. Volkov, and K.B. Efetov, *ibid.* **77**, 1321 (2005).
 [7] T. Novotny, A. Rossini, and K. Flensberg, *Phys. Rev. B* **72**, 224502 (2005); J. Sköldbberg, T. Löfwander, V.S. Shumeiko, and M. Fogelström, *Phys. Rev. Lett.* **101**, 087002 (2008).
 [8] A. Zazunov, R. Egger, C. Mora, and T. Martin, *Phys. Rev. B* **73**, 214501 (2006); A. Zazunov, D. Feinberg, and T. Martin, *Phys. Rev. Lett.* **97**, 196801 (2006).
 [9] W.H.A. Thijssen *et al.*, *Phys. Rev. Lett.* **97**, 226806 (2006).
 [10] A.V. Danilov *et al.*, *Nano Lett.* **6**, 2184 (2006).
 [11] A. Donarini, M. Grifoni, and K. Richter, *Phys. Rev. Lett.* **97**, 166801 (2006); A. Mitra and A.J. Millis, *Phys. Rev. B* **76**, 085342 (2007).
 [12] P. Lucignano, G.E. Santoro, M. Fabrizio, and E. Tosatti, *Phys. Rev. B* **78**, 155418 (2008).
 [13] Consider the dot in Eq. (1) capacitively side-coupled to a double dot (fermion operators $f_{1,2}$) tuned to single occupancy, $f_1^\dagger f_1 + f_2^\dagger f_2 = 1$. Then the TLS-plus-coupling part of H_0 is $-\frac{W_0}{2}(f_1^\dagger f_2 + f_2^\dagger f_1) - \frac{E_0}{2}(f_1^\dagger f_1 - f_2^\dagger f_2) + \sum_{i=1,2} U_i f_i^\dagger f_i (n_\uparrow + n_\downarrow)$, and λ corresponds to the difference in capacitive couplings $U_1 - U_2$.
 [14] W. Zhang and X. Zhang, *Prog. Polymer Sci.* **28**, 1271 (2003).
 [15] The generalization to asymmetric cases is straightforward and does not yield new physics.
 [16] F. Hekking and Yu.V. Nazarov, *Phys. Rev. B* **44**, 11506 (1991); L.Y. Gorelik *et al.*, *Phys. Rev. Lett.* **75**, 1162 (1995); D.V. Averin and A. Bardas, *ibid.* **75**, 1831 (1995).
 [17] A.L. Yeyati, A. Martín-Rodero, and E. Vecino, *Phys. Rev. Lett.* **91**, 266802 (2003).
 [18] A. Zazunov *et al.*, *Phys. Rev. Lett.* **90**, 087003 (2003); A. Zazunov, V.S. Shumeiko, G. Wendin, and E.N. Bratus', *Phys. Rev. B* **71**, 214505 (2005).